Biosensor-enabled on-site therapeutic drug monitoring of antibiotics

Can Dincer (dincer@imtek.de)
University of Freiburg https://orcid.org/0000-0003-3301-1198

Hatice Ceren Ates
University of Freiburg

Hasti Mohsenin
University of Freiburg

Christin Wenzel
University Medical Center Freiburg https://orcid.org/0000-0002-8910-9904

Regina Glatz
University of Freiburg

Hanna Wagner
University of Freiburg https://orcid.org/0000-0003-4203-4949

Richard Bruch
University of Freiburg

Nico Höfflin
University of Freiburg

Sashko Spassov
University Medical Center Freiburg https://orcid.org/0000-0002-3585-3682

Lea Streicher
University of Freiburg

Sara Lozano-Zahonero
University Medical Center Freiburg

Bernd Flamm
University of Freiburg

Maja Köhn
University of Freiburg https://orcid.org/0000-0001-8142-3504

Johannes Schmidt
University of Freiburg

Stefan Schumann
University Medical Center Freiburg https://orcid.org/0000-0003-0773-7489

Gerald Urban
University of Freiburg

Wilfried Weber

University of Freiburg

Article

Keywords: Drug monitoring, ß-lactam antibiotics, exhaled breath condensate, personalized antibiotherapy, non-invasive diagnostics, multiplexing, point-of-care testing, wearables

Posted Date: May 11th, 2021

DOI: https://doi.org/10.21203/rs.3.rs-429808/v1

Abstract

Antimicrobial resistance is increasing with an alarming rate for which the prime suspect is the “one size-fits-all” dosage strategies of antibiotics. Personalized antibiotherapy framework appears as a viable option to counteract inadequate dosage, as it offers the application of the optimal dosage regimen for each individual. Such individualized scheme, however, needs frequent sampling to tailor the blood antibiotic concentration to respond unique pharmacokinetic/pharmacodynamic (PK/PD) of the patient. Herein, there are two alternative paths for feasible therapeutic drug monitoring (TDM); transforming our understanding to utilize blood based sampling within the scope of point-of-care (POC), or focusing on non-invasive samples. Here, we present a versatile biosensor along with an antibody-free assay that can be utilized in both paths for on-site TDM. The developed platform is evaluated in a large animal study (pigs exposed with overdose, normal dose, and underdose of ß lactams), in which antibiotic concentrations are quantified in matrices including whole blood, plasma, urine, saliva, and exhaled breath condensate (EBC). Herein, the detection and the clearance of drug concentrations in EBC is demonstrated for the first time. Influence of the secretion mechanisms on measured drug concentrations is then quantified by comparing the plasma concentrations with those in EBC, saliva and urine. The potential of the developed platform for blood-based POC application is further illustrated by tracking ß lactam concentrations in untreated blood samples. Finally, multiplexing capabilities are explored successfully for multianalyte/sample analysis. Enabling a rapid, low-cost, sample-independent, and multiplexed on-site TDM, this system could pave the way for the personalized drug therapies and thus, shift the paradigm of “one size-fits-all” strategies.

Introduction

We are at risk of losing the power of antibiotics, as the antimicrobial resistance is rising to dangerous levels. Newly developed agents are becoming ineffective much more rapidly than during the previous decades, while the celerity of our new inventions alarmingly falls behind. This bottleneck mandates the re-evaluation of our battle strategy about how we utilize the existing antibiotics.

Success of the antibiotherapy strongly depends on the ability to keep the antibiotic concentrations in the blood within therapeutic ranges tailored to respond the unique pharmacokinetic/pharmacodynamics (PK/PD) of the patient. In the current practice, however, this operational window is determined based on the data collected from animal models and healthy population. Based on these statistically accepted ranges, patients´ drug concentrations are then categorized as either subtherapeutic, therapeutic, or toxic. Therefore, physicians can only judge the presence or absence of a clinical response days later and then new dosage regimens are recommended to adjust the serum concentrations.[1] In this regard, traditional therapeutic drug monitoring (TDM) would be an extension of the “one-size-fits-all” approach, potentially resulting in sub-therapeutic conditions and in turn, antibiotic resistance.[1–5] Given the variations in the antibiotic exposures across different patients, personalized antibiotherapy is considered as a promising remedy to maximize the antibiotic effectiveness. In such an individualized approach, the dynamics of the treatment process is to be tailored simultaneously, according to the requirements of each individual.[1]

This process necessitates a feedback control loop, bringing a much greater burden to the clinical laboratory because samples need to be analyzed more frequently to tailor both the PK/PD models and the therapeutic targets.

Therapeutic studies have been mostly established for blood-based measurements providing a voluminous database of clinical relevance. Nonetheless, this familiar approach is impractical considering the cost and resources associated with collecting, transporting, processing, and analysing the blood for personalized TDM. Recent blood-based studies are focusing on ways to alleviate these issues by decreasing the sample volume and eliminating the need for an expensive equipment and expertise.[6–11] The other path includes the utilization of alternative matrices such as interstitial fluid[12–18], tears[19], saliva[20–22], sweat[22–29] to replace the invasive TDM. Herein, the common challenges stem from the complex transport mechanisms of antibiotics from the blood to the sampling site of interest, which makes the interpretation of the measured concentrations unique for each medium. Breath could be a potential alternative to bypass the transportation-related issues, as blood-breath transportation is relatively direct compared with the other non-invasive samples. In particular, transport resistances result in low analyte concentrations necessitating highly sensitive detection methods, while secretion of the non-invasive samples further complicates the way the antibiotics interacts with metabolic activities. Consequently, there is still no consensus in the community on how to interpret the measured concentrations and how to correlate them with blood-based measurements. In clinical practice, this uncertainty is translated into the following questions: (i) can we measure the antibiotic concentrations sensitive enough to perform PK/PD analysis? (ii) how can we identify the effect of transport mechanisms on measured concentrations? and (iii) can we quantify the instantaneous correlation between blood and non-invasive samples, preferably on the same platform? To answer these questions, we introduce a versatile, polymer-based, disposable microfluidic sensor along with an antibody-free and highly sensitive ß-lactam assay (**Figure 1**) and explore its capabilities with animal experiments conducted on Landrace pigs treated with three different (under-, over- and normal) dosages of piperacillin/tazobactam. We successfully demonstrate, for the first time, the detection and temporal monitoring of piperacillin/tazobactam concentrations in plasma and exhaled breath condensate (EBC). We further examine the impact of secretion mechanisms by comparing plasma concentrations with those in EBC, saliva, and urine. We then survey the possibility of tracking concentration variations in untreated whole blood samples to explore the potential of our implemented biosensing system for POC applications. Finally, we present the multiplexing capability of our technology as a potential platform to generate a cross-correlation database via ß-lactam measurements in plasma, EBC, saliva, and urine simultaneously on the same chip.

Methods

The microfluidic biosensor was manufactured by using the dry film photoresist (DFR) technology.[30] Multiple DFR layers were stacked onto a platinum-patterned polyimide substrate, on which the microchannels and electrodes are realized (**Supporting Information**). Each biosensor consists of two

consecutive zones; an immobilization area and an electrochemical cell, which are separated by a hydrophobic stopping barrier to prevent electrode fouling. Sample containing the analyte first goes through the immobilization area by capillary forces, in which competitive binding between the analyte (ß-lactam in the sample) and ampicillin-biotin conjugate to Penicillin binding protein-3 (PBP-3) takes place (**Table S2, Supporting Information**). Streptavidin-glucose oxidase (Str-GOx) is utilized as a detection enzyme converting glucose to hydrogen peroxide (H_2O_2). The signal transduction is achieved through the detection of the generated H_2O_2 in the electrochemical cell using a platinum working and counter electrode together with a silver/silver chloride reference electrode.

For the electrochemical readout, a glucose solution (40 mM glucose in 10 mM PBS) was pumped through the microfluidic sensor, which is catalysed on the functionalized surface by GOx. Produced H_2O_2 was amperometrically detected at the Pt working electrode by using fully automated stop-flow technique for signal amplification (**Figure S11, Supporting Information**). Herein, the signal is directly proportional to the amount of immobilized GOx and therefore, inversely proportional to the ß-lactam concentration in the sample. In this work, the assay stability was improved by redesigning the PBP-3 and ampicillin-biotin conjugate[10] (**Figure S1-2, Supporting Information**) and optimizing each assay component with respect to incubation time and concentration using an alternative surface blocker (**Figure S4-9, Supporting Information**). Improved assay yielded a limit-of-detection (LOD) of 56 ng ml^{-1} by fitting the measured data points to a four parametric sigmoidal curve (**Figure S10, Supporting Information**) with a wide operational window up to 1000 µg ml^{-1} and a sample-to-result time less than 90 minutes.

For both blood-based and non-invasive samples, German Landrace hybrid pigs with a weight of 43 ± 3 kg (6 males, 3 females) were used. Piperacillin/tazobactam was injected intravenously with either 200%, 100% or 50% of the standard dose (4 g piperacillin / 0.5 g tazobactam). Samples of blood, saliva and urine were taken before (ST), 5 (BL), 30, 60, 120, 180 and 240 minutes after administration of antibiotics. Expiratory gas is drawn from the airway's mainstream and cooled down at –7.5 °C for condensation. The EBC samples were collected before injection of antibiotics, 30, 60, 120, 180 and 240 minutes after (**Figure S3, Supporting Information**). In the sample pre-processing step, collected raw samples were diluted via a dilution factor optimized for each sample type (**Figure S12-14, Supporting Information**). Measured current density was also converted to free drug concentrations to highlight the quantitative nature of developed strategy by using the calibration curve generated with PBS samples spiked with different concentrations of piperacillin / tazobactam (**Figure S10, Supporting Information**).

Results

Utilization of EBC analysis is a promising yet rather unexplored alternative for personalized antibiotherapy. In this study, we first explored the possibility of bypassing transportation related issues by using EBC since the blood-EBC transfer offers a more direct contact comparing to other non-invasive alternatives. **Figure 2** demonstrates the measured course of piperacillin/tazobactam concentrations in plasma and EBC for overdose, normal dose, and underdose scenarios. In all cases, similar clearance

behavior (sudden decrease followed by a stepwise increase in current density) was observed for both plasma and EBC measurements. To our best knowledge, this is the first successful demonstration of the detection and clearance of antibiotic concentrations in EBC samples.

The measured concentration in plasma immediately after the drug infusion (Baseline-BL) reflected the dosage regimen (over-normal-under), in average dropping from 6,600 to 1,700 to 300 µg ml^{-1} (**Figure 2d-f**). Furthermore, antibiotic clearance over time could be tracked for each individual case (over-normal-under). Nonetheless, there was a striking variance in the rate of drug clearance between the different pigs at a given time. For instance, plasma concentration measured at 60 minutes was found to be highest for the normal-dosed animals. EBC measurements further revealed that there is a 4-order of magnitude decrease in the measured drug concentrations (from 308 µg ml^{-1} to 93 ng ml^{-1} for overdosed animal, for example), validating the expected concentration drop during the analyte transfer from the blood stream to aerosol particles.[31] Interestingly, antibiotic concentrations found at 30 minutes were consistently around 90 ng ml^{-1}. Considering the time, it takes to collect breath condensates (also 30 minutes), this very first sample included the total amount of antibiotics transferred to the aerosols from the beginning of the drug infusion. Since the plasma concentrations after 30 minutes were found to be significantly different (**Figure 2d-f**), this upper limit in EBC concentrations may indicate a saturation of transport capacity through capillary walls, interstitial space, or epithelial cells (**Figure 3f**).

Next, we examined the impact of secretion mechanisms by comparing the plasma concentrations with those in EBC, saliva, and urine for an animal given an overdose of piperacillin/tazobactam (**Figure 3**). The clearance behavior observed in plasma was reflected by both EBC and saliva during the measurement period of 3 hours. The rate of change of drug concentrations in EBC and saliva exhibited almost identical trends (**Figure 3c**). In the case of urine, however, the first antibiotic detection occurred after 3 hours indicating a significant process delay. The striking similarity between EBC and saliva concentration profiles (exponential decay) might be related to how we access the antibiotic carrier medium (**Figure 3c**). Whole saliva was made of secretions from various glands, accumulating within the salivary ducts.[1,32,33] Antibiotics passing from the blood stream to the saliva were mixed and diluted within these ducts and then withdrawn from this “chamber” (**Figure 3f**). As a result, the concentration in the saliva reflects the history of drug transportation at a given time giving a cumulative (residence time) information rather than an instantaneous feedback. In fact, this natural process was mimicked in the EBC collection procedure, where sample collection takes 30 minutes (**Figure S3 Supplementary Information**). In our opinion, these similarities between measured concentration trends originate from this natural (salivary glands)/artificial (EBC collector) sample collection procedure.

Following the analysis of potential utilization of non-invasive samples in personalized antibiotherapy, we surveyed the possibility of tracking concentration variations in untreated whole blood samples, with the vision of a TDM platform similar to blood glucometers for POC applications. Blood samples collected from three different pigs given overdose, normal dose, and underdose of ß-lactam antibiotic were analyzed by using the same microfluidic platform (**Figure 4**). The applicability of the proposed system

could be successfully demonstrated without any matrix effect and with a clearance behavior similar to the plasma measurements (**Figure 4a-c**). Furthermore, drug concentrations followed the dosage regimen quantitatively. Nonetheless, during the concentration measurements, one anomaly was detected at around 120 minutes for the normal-dosed animal (**Figure 4b**). This time point correlated with an emergency dosage of propofol (an anesthetic drug) to maintain anesthesia of the animal. An additional test with a whole blood sample spiked with a similar concentration of propofol confirmed the hypothesis of drug interference (**Figure S15, Supplementary Information**).

Observing multidrug interference and its impact on the quantitative analysis, we investigated the multiplexing capability of our technology as a potential platform to generate cross-correlation database (**Figure 5**). On the multiplexed biosensor chip (Biosensor X), there are four functionalized zones coupled with their own electrochemical cells (**Figure 5a-b**).[34,35] In Biosensor X, each incubation area is followed by individual electrochemical cell, resulting in successive peaks by using stop-flow measurement (**Figure 5c**). With this architecture, it is possible to combine (i) different assays for multianalyte measurements in a given medium (simultaneous measurement of ß-lactams and sepsis biomarkers like inflammation markers), (ii) multi-sample measurements over the same assay (piperacillin/tazobactom measurement in different sample types), or (iii) a combination of both.

In this study, we performed a baseline measurement of the optimized assay with plasma, EBC, urine, and saliva samples, demonstrating the proof-of-principle of this approach (**Figure 5d**). However, with the current design of Biosensor X, we encountered overflow of biomolecules between consecutive incubation steps. Consequently, we observed a significant variation in the current densities during our measurements. The next step will be the optimization of the microfluidic chip design to solve the aforementioned issues and further investigation of the change in drug concentrations under different dosage regimens, a step towards on-site TDM for personalized antibiotherapy.

Discussion

In the current context of clinical TDM, drug concentration measurements are performed by using either chromatographic methods or immunoassays, hence limiting the large scale, distributed TDM practice.[1,33] In this regard, our platform offers an opportunity to explore the full potential of personalized antibiotherapy by providing (i) a rapid (sample-to-result time less than 90 minutes) and low-cost solution for quantitative measurement, (ii) information about “free” drug concentration without any sample pre-treatment, and (iii) the potential for simultaneously measuring different targets without compromising its simplicity. The proposed system is versatile with its wide operational window (measurement range spanning from ng ml^{-1} to µg ml^{-1} with a LOD of 56 ng ml^{-1}) and can be used for antibiotic quantification in different sample types. In a typical electrochemical sensor, biomolecules for signal generation are immobilized on the electrode surface, which requires additional precautions such as protective coating to minimize the fouling caused by complex biofluids.[36] In our system, we inherently bypass the fouling issue, as we separated the immobilization zone and the electrochemical cell with a hydrophobic barrier (**Figure 1** and **Supporting Information**). This design strategy enables us to work with complex biofluids

such as whole blood without compromising sensitivity. We also tested the possibility of measuring complex biofluids on the same chip simultaneously by using our multiplexed chip, Biosensor X. Although we show that it is possible to measure four different analytes, we observe some design-related issues during the functionalization of the biosensor between consecutive incubation steps. We noticed that overflow of biomolecules occurred due to (i) insufficient Teflon barrier size and (ii) the position of the inlet hole. In the current Biosensor X design, the individual inlet holes were placed in the middle of the channel to ensure homogenous biomolecule immobilization throughout the channel. However, this arrangement complicated the handling during incubation and created a redundant load on the hydrophobic barriers. Our future goal is to improve the design to make it more “user-friendly”.

Our observations reveal that there are distinct clearance behaviors for different mediums in accordance with their complex transport mechanisms. In principle, blood-EBC antibiotic transfer is expected to be more direct through capillary walls densely surrounding alveoli (**Figure 3f**). This potential of instantaneous access, however, is very difficult to realize in practice. If the exhaled breath condensate is collected in an external cooled chamber over a period of time, which was the case in our study, the accessible information from EBC involves a time delay and a history of concentration changes. As a remedy, alternative strategies can be utilized such as wearable breath sensors including facemasks, in-mouth/in-nose implants, or augmented sensing platforms exploiting natural sensors in respiratory tract.[37] In this case, however, the sensor should be sensitive and selective enough to detect the analyte within more than 3,000 volatile organic compounds in the presence of other exogenous effects.[1] Therefore, in our opinion, the near-future potential of exhaled breath for personalized antibiotherapy lies in multi-sample framework, providing additional insights into metabolic activities. In the light of the knowledge acquired in this work, one of our future work will be the extension of our paper-based wearable sensor[38], which can be integrated onto any type of facemasks, for the real-time and continuous measurement of ß-lactam antibiotics from exhaled breath.

Transport dynamics into saliva glands depend on the dissociation constant, lipophilicity, pH, protein binding affinity and ionizability of the drug[1,33], and thus can be much more complex than capillary diffusion through alveoli (**Figure 3f**). Our saliva and EBC measurements yielded a similar exponential decay (**Figure 3d**), indicating that piperacillin/tazobactom transfer from blood to collected saliva was not influenced significantly by these inherent complexities. This outcome shows the potential of our sensor for personalized saliva-based ß-lactam monitoring. Urine goes through even a more complicated cycle, which composes a very rich sample which contains urea, creatinine, ammonia, uric acid, blood cells, hormones, bilirubin, amino acids, proteins, sulphate, phosphate, chloride, sodium, potassium and other trace elements. Therefore, urine analysis is typically prone to low signal-to-noise ratio due to the matrix effect. In our platform, we alleviated this issue by working with diluted urine samples, for which the assay sensitivity was optimized to be functional at very low concentrations. During the experiments, we did not observe any decrease in the current density for the first five measurements, which is followed by a sharp decrease indicating the presence of ß-lactam in urine (**Figure 3d**).

Another important use case for the developed sensor is the whole blood measurements, which enables an easy access to pharmacokinetically relevant information such as inter-patient variance, effect of external factors, and dosage. The success of the antibiotherapy heavily depends on keeping the blood antibiotic concentrations within the therapeutic range and this range must be tailored to respond unique PK/PD of the patient. Such individualization process, however, requires frequent sampling. Herein, low volume requirement and the ability to process untreated whole blood with the proposed sensor may catalyze the realization of on-site TDM. This is of particular importance for specific patient groups like pediatric, neonatal, and elderly patients, for whom repetitive blood collection via venipuncture is difficult. With a further improvement of the design and integrating all necessary components in one handheld device, it could be possible to utilize our platform for decentralized TDM, similar to the diabetes monitoring via blood glucometer.

Alternative samples offer a great potential for a wide range of future on-site TDM applications. In the clinical practice, however, there are many uncertainties regarding the diagnostic correspondence of the measured concentrations in non-invasive samples and how these concentrations are correlated to the more familiar blood-based counterparts. Unfortunately, a direct correlation between a non-invasive sample and blood for a given analyte (piperacillin/tazobactom) is hard to formulate mainly due to the nonlinear transport mechanisms, which is further complicated by inter-patient variance and exogenous factors. Our observations demonstrate that we need to include more animals in our study to create a “database”, which may reveal the unknown link between blood and non-invasive matrices. This study could also be supported in the future with a prospective and observational pharmacokinetic study in patient populations. Consequently, multiplexed sensing can help to improve the overall reliability of the system by providing a physiological information for active calibration and correction of target concentrations.[33,39] Therefore, any proposed remedy has to be simple, fast, and economical enough to make therapeutic drug management decentralized. In this work, we responded to this call by implementing a versatile platform that can operate with multianalyte/sample tasks. A successful realization of either blood-based or non-invasive on-site monitoring of antibiotics using such a biosensor could be a game-changer in the antibiotherapy in the longer run and beyond since this technology could be extended to measure other drugs and biomarkers[40]. For instance, combining TDM of antibiotics and inflammation progress biomarkers could pave the way to personalized antibiotherapy.[41,42] This could be a significant landmark on the global combat against antibiotic resistances.

Declarations

Experimental Section

Details of the experiments and methods described in the Supporting Information.

Acknowledgements

The authors would like to thank the Deutsche Forschungsgemeinschaft (DFG, German Research Foundation) for funding this work under grant number 404478562 and Germany's Excellence Strategy CIBSS - EXC-2189 - Project ID: 390939984. The authors also thank Isabel Busam for helping with protein production and purification.

Conflict of Interest

The authors declare no conflict of interest.

References

1. Ates, H. C. *et al.* On-Site Therapeutic Drug Monitoring. *Trends Biotechnol.* **38**, 1262–1277 (2020).
2. Roberts, J. A. *et al.* Therapeutic drug monitoring of β-lactams in critically ill patients: Proof of concept. *Int. J. Antimicrob. Agents* **36**, 332–339 (2010).
3. Wong, G. *et al.* Therapeutic drug monitoring of b-lactam antibiotics in the critically ill: Direct measurement of unbound drug concentrations to achieve appropriate drug exposures. *J. Antimicrob. Chemother.* **73**, 3087–3094 (2018).
4. Jelliffe, R., Neely, M. & Bayard, D. Pharmacokinetic methods for TDM data analysis and optimal individualization of drug dosage regimens. in *Handbook of Analytical Separations* **7**, 135–168 (2020).
5. Jelliffe, R. W. & Neely, M. *Individualized Drug Therapy for Patients*. *Chapter 1 - Basic Pharmacokinetics and Dynamics for Clinicians* (Elsevier, 2017). doi:10.1016/c2014-0-03786-0
6. Weber, J. *et al.* Validation of a dried blood spot method for therapeutic drug monitoring of citalopram, mirtazapine and risperidone and its active metabolite 9-hydroxyrisperidone using HPLC–MS. *J. Pharm. Biomed. Anal.* **140**, 347–354 (2017).
7. Dauphin-Ducharme, P. *et al.* Electrochemical Aptamer-Based Sensors for Improved Therapeutic Drug Monitoring and High-Precision, Feedback-Controlled Drug Delivery. *ACS Sensors* **4**, 2832–2837 (2019).
8. Ceren Ates, H. *et al.* Personalized antibiotherapy via ⁓finger prick⁓ blood test. in *MicroTAS 2020 - 24th International Conference on Miniaturized Systems for Chemistry and Life Sciences* (2020).
9. Chien, J. C., Baker, S. W., Soh, H. T. & Arbabian, A. Design and Analysis of a Sample-and-Hold CMOS Electrochemical Sensor for Aptamer-Based Therapeutic Drug Monitoring. *IEEE J. Solid-State Circuits* **55**, 2914–2929 (2020).
10. Bruch, R. *et al.* Clinical on-site monitoring of ß-lactam antibiotics for a personalized antibiotherapy. *Sci. Rep.* **7**, 1–10 (2017).
11. Kling, A. *et al.* Multianalyte Antibiotic Detection on an Electrochemical Microfluidic Platform. *Anal. Chem.* **88**, 10036–10043 (2016).
12. Gowers, S. A. N. *et al.* Development of a Minimally Invasive Microneedle-Based Sensor for Continuous Monitoring of β-Lactam Antibiotic Concentrations in Vivo. *ACS Sensors* **4**, 1072–1080

(2019).

13. Rawson, T. M. *et al.* Towards a minimally invasive device for beta-lactam monitoring in humans. *Electrochem. commun.* **82**, 1–5 (2017).
14. Ranamukhaarachchi, S. A. *et al.* Integrated hollow microneedle-optofluidic biosensor for therapeutic drug monitoring in sub-nanoliter volumes. *Sci. Rep.* **6**, 1–10 (2016).
15. Rawson, T. M. *et al.* Microneedle biosensors for real-time, minimally invasive drug monitoring of phenoxymethylpenicillin: a first-in-human evaluation in healthy volunteers. *Lancet Digit. Heal.* **1**, 335–343 (2019).
16. Kiang, T. K. L. *et al.* Revolutionizing therapeutic drug monitoring with the use of interstitial fluid and microneedles technology. *Pharmaceutics* **9**, 1–21 (2019).
17. Sempionatto, J. R. *et al.* An epidermal patch for the simultaneous monitoring of haemodynamic and metabolic biomarkers. *Nat. Biomed. Eng.* 1–12 (2021).
18. Wang, Z. *et al.* Microneedle patch for the ultrasensitive quantification of protein biomarkers in interstitial fluid. *Nat. Biomed. Eng.* **5**, 64–76 (2021).
19. Yamada, K., Yokoyama, M., Jeong, H., Kido, M. & Ohno, Y. Paper-based surfaced enhanced Raman spectroscopy for drug level testing with tear fluid. in *Optics InfoBase Conference Papers* (SPIE, 2014).
20. Ventura, S., Rodrigues, M., Pousinho, S., Falcão, A. & Alves, G. Determination of lamotrigine in human plasma and saliva using microextraction by packed sorbent and high performance liquid chromatography–diode array detection: An innovative bioanalytical tool for therapeutic drug monitoring. *Microchem. J.* **130**, 221–228 (2017).
21. Ghareeb, M., Gohh, R. Y. & Akhlaghi, F. Tacrolimus Concentration in Saliva of Kidney Transplant Recipients: Factors Influencing the Relationship with Whole Blood Concentrations. *Clin. Pharmacokinet.* **57**, 1199–1210 (2018).
22. Lin, S. *et al.* Noninvasive wearable electroactive pharmaceutical monitoring for personalized therapeutics. *Proc. Natl. Acad. Sci. U. S. A.* **117**, 19017–19025 (2020).
23. Brasier, N. *et al.* Non-invasive Drug Monitoring of β-Lactam Antibiotics Using Sweat Analysis—A Pilot Study. *Front. Med.* **7**, 476 (2020).
24. Brasier, N. *et al.* The Detection of Vancomycin in Sweat: A Next-Generation Digital Surrogate Marker for Antibiotic Tissue Penetration: A Pilot Study. *Digit. Biomarkers* **5**, 24–28 (2021).
25. Lin, S. *et al.* Design Framework and Sensing System for Noninvasive Wearable Electroactive Drug Monitoring. *ACS Sensors* **5**, 265–273 (2020).
26. Tai, L. C. *et al.* Methylxanthine Drug Monitoring with Wearable Sweat Sensors. *Adv. Mater.* **30**, 1–8 (2018).
27. Tai, L. C. *et al.* Wearable Sweat Band for Noninvasive Levodopa Monitoring. *Adv. Healthc. Mater.* **4**, 1–8 (2019).

28. Koh, E. H. *et al.* A Wearable Surface-Enhanced Raman Scattering Sensor for Label-Free Molecular Detection. *ACS Appl. Mater. Interfaces* **13**, 3032 (2021).
29. Criscuolo, F. *et al.* Wearable multifunctional sweat-sensing system for efficient healthcare monitoring. *Sensors Actuators, B Chem.* **328**, 129017 (2021).
30. Bruch, R., Kling, A., Urban, G. A. & Dincer, C. Dry Film Photoresist-based Electrochemical Microfluidic Biosensor Platform: Device Fabrication, On-chip Assay Preparation, and System Operation. *J. Vis. Exp.* 1–7 (2017).
31. Effros, R. M. *et al.* A Simple Method for Estimating Respiratory Solute Dilution in Exhaled Breath Condensates. *Am. J. Respir. Crit. Care Med.* **168**, 1500–1505 (2003).
32. Gug, I. T., Tertis, M., Hosu, O. & Cristea, C. Salivary biomarkers detection: Analytical and immunological methods overview. *TrAC - Trends Anal. Chem.* **113**, 301–316 (2019).
33. Ates, H. C. *et al.* Integrated Devices for Non-Invasive Diagnostics. *Adv. Funct. Mater.* 2010388 (2021).
34. Bruch, R. *et al.* CRISPR-powered electrochemical microfluidic multiplexed biosensor for target amplification-free miRNA diagnostics. *Biosens. Bioelectron.* **177**, 112887 (2021).
35. Dincer, C., Kling, A., Urban, G. A. & Bruch, R. Single-Channel Multianalyte Biosensor. (2019). doi:WO 2019/134741 A1
36. Hanssen, B. L., Siraj, S. & Wong, D. K. Y. Recent strategies to minimise fouling in electrochemical detection systems. *Reviews in Analytical Chemistry* **35**, 1–28 (2016).
37. Ates, H. C., Yetisen, A. K., Güder, F. & Dincer, C. Wearable devices for the detection of COVID-19. *Nat. Electron.* **4**, 13–14 (2021).
38. Maier, D. *et al.* Toward Continuous Monitoring of Breath Biochemistry: A Paper-Based Wearable Sensor for Real-Time Hydrogen Peroxide Measurement in Simulated Breath. *ACS Sensors* **4**, 2945–2951 (2019).
39. Dincer, C., Bruch, R., Kling, A., Dittrich, P. S. & Urban, G. A. Multiplexed Point-of-Care Testing – xPOCT. *Trends Biotechnol.* **35**, 728–742 (2017).
40. Michael, I. *et al.* A fidget spinner for the point-of-care diagnosis of urinary tract infection. *Nat. Biomed. Eng.* **4**, (2020).
41. Reddy, B. *et al.* Point-of-care sensors for the management of sepsis. *Nat. Biomed. Eng.* **2**, 640–648 (2018).
42. Park, S. min *et al.* A mountable toilet system for personalized health monitoring via the analysis of excreta. *Nat. Biomed. Eng.* **4**, 624–635 (2020).

Figures

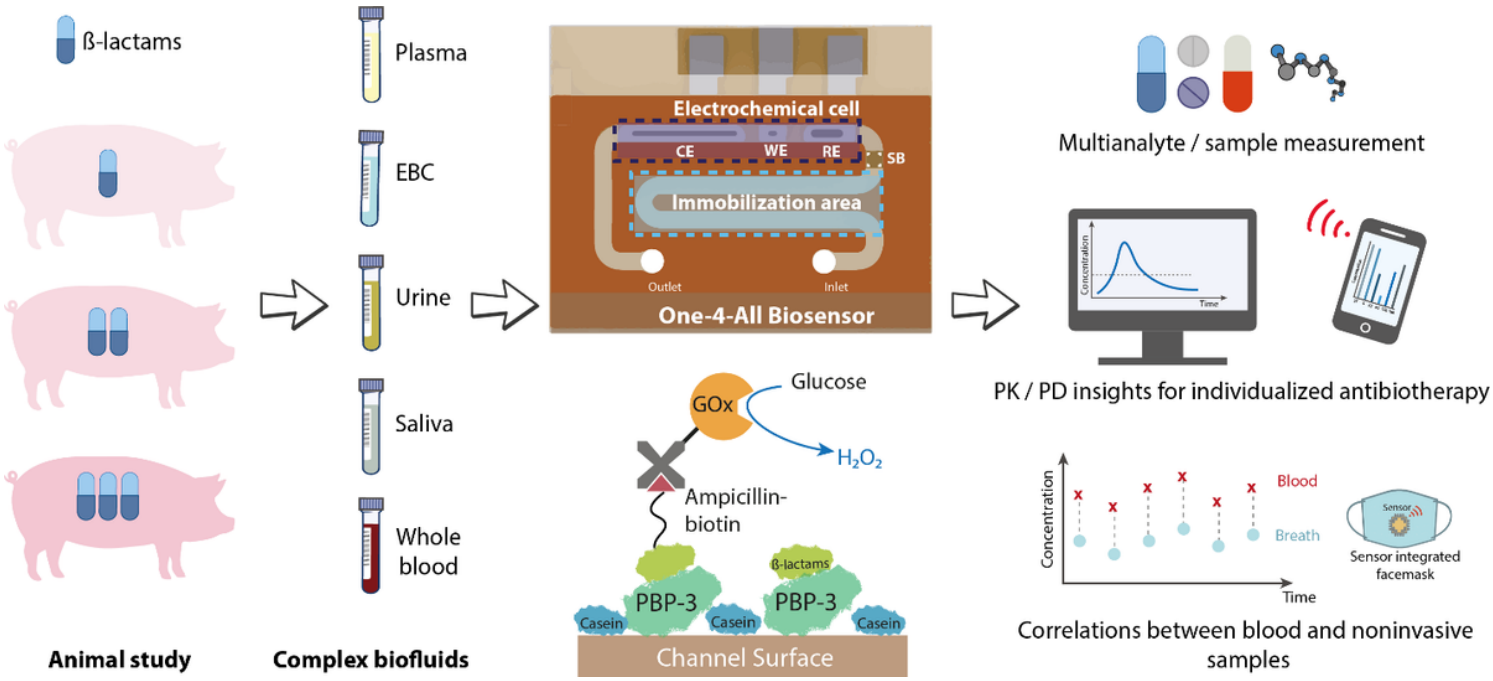

Figure 1

Utilization of proposed biosensor with the envisioned POC scenario. Both invasive and non-invasive samples collecting from landrace pigs given overdose, normal dose and underdose piperacillin/tazobactam are analyzed using our electrochemical biosensor. The microfluidic chip used consists of two consecutive zones separated by a hydrophobic stopping barrier. By separating electrochemical detection zone from immobilization area, our platform can bypass the electrode fouling issue and operate with complex biofluids, like whole blood. A competitive and antibody-free assay using penicillin-binding proteins enables a rapid (less than 90 minutes) and highly sensitive (ng ml−1 range) detection of ß-lactams. Combining with multiplexed microfluidics, our biosensor has the potential to be used in multianalyte/sample measurements as well as PK/PD and correlations studies for individualized drug therapy.

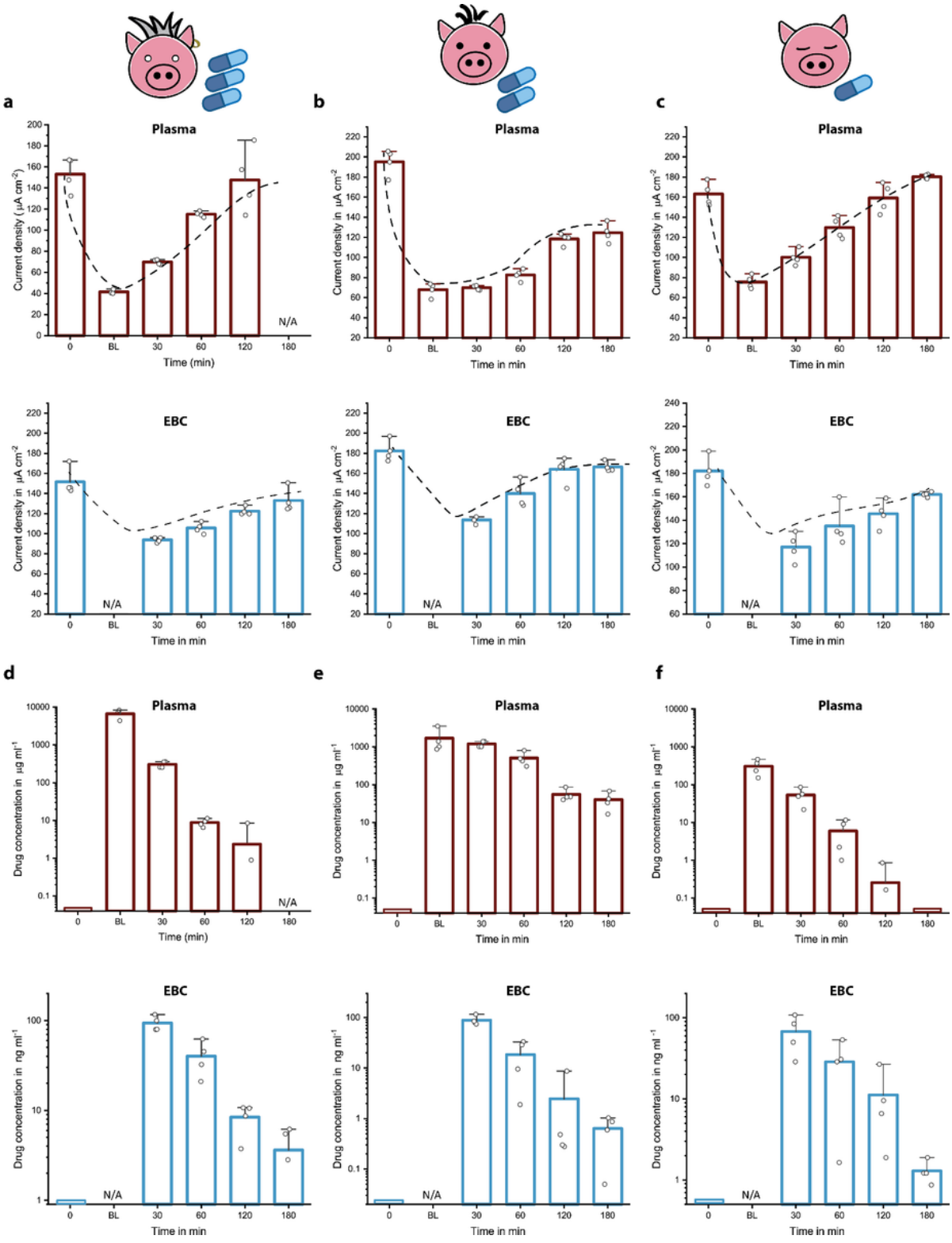

Figure 2

Measured current densities (a-c) and calculated free drug concentrations (d f) for plasma and EBC samples of animals given overdose, normal dose, and underdose piperacillin/tazobactam. A similar clearance behavior and expected concentration decrease with respect to drug dosing regimen were observed for both plasma and EBC measurements over a time period starting from before antibiotic administration (0), after 5 (BL), 30, 60, 120 and 180 minutes. For EBC measurements, the collection time

is 30 minutes and thus, the first samples were collected at t = 30. For overdose animal, no plasma sample was collected at t = 180. Box and whisker plot for n = 4 replicates. Error bars represent the outlier range.

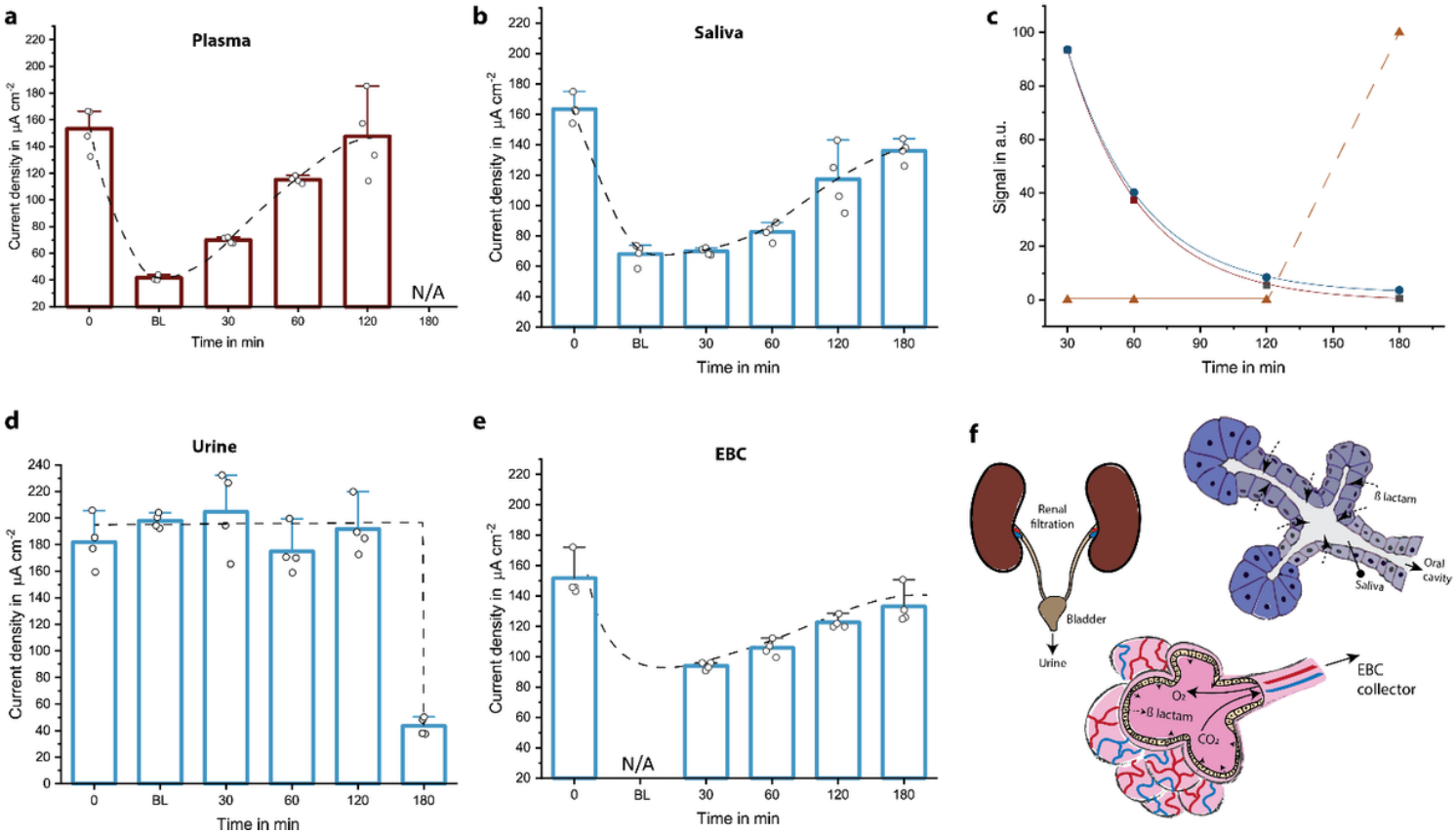

Figure 3

Demonstration of the measured current densities over a time period starting from before antibiotic administration (0), after 5 (BL), 30, 60,120 and 180 minutes for plasma (a), saliva (b), urine (d), and EBC (e) samples of animals given overdose piperacillin/tazobactam (a-d). The drug concentration profiles for non invasive samples revealing the decay in drug concentrations (c), and overview of drug transport mechanisms from blood to these samples. (f) Secretion mechanisms of alternative matrices. Box and whisker plot for n = 4 replicates. Error bars represent the outlier range.

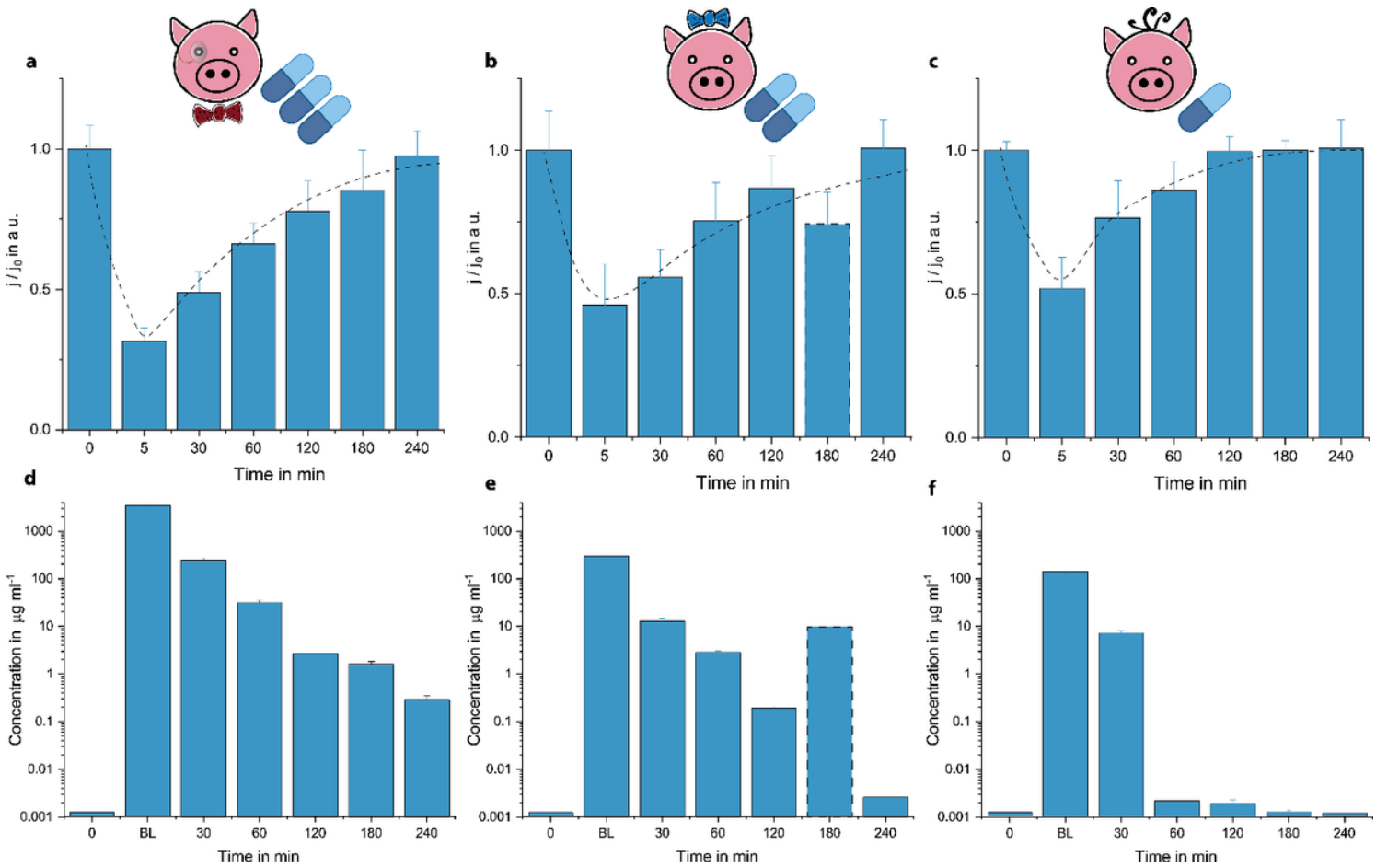

Figure 4

Multianalyte/sample capability of the proposed biosensing technology. (a) 3D rendering of the stacked multiplexed biosensor (Biosensor X) and (b) four different incubation areas, individual electrochemical cells and Teflon barriers preventing electrode fouling. (c) Amperometric signal readout. The first four successive peaks correspond to the accumulation of electrochemically active species in the immobilization area during stop-flow protocol. During the “flow” phase, these species are passing through neighboring electrochemical cells in addition to their own individual electrochemical cell, which creates the following faint peaks. (d) Demonstration of the proof of principle via measuring four different sample types on the single-channel multiplexed biosensor. Box and whisker plot for n = 3 replicates. Error bars represent the outlier range.

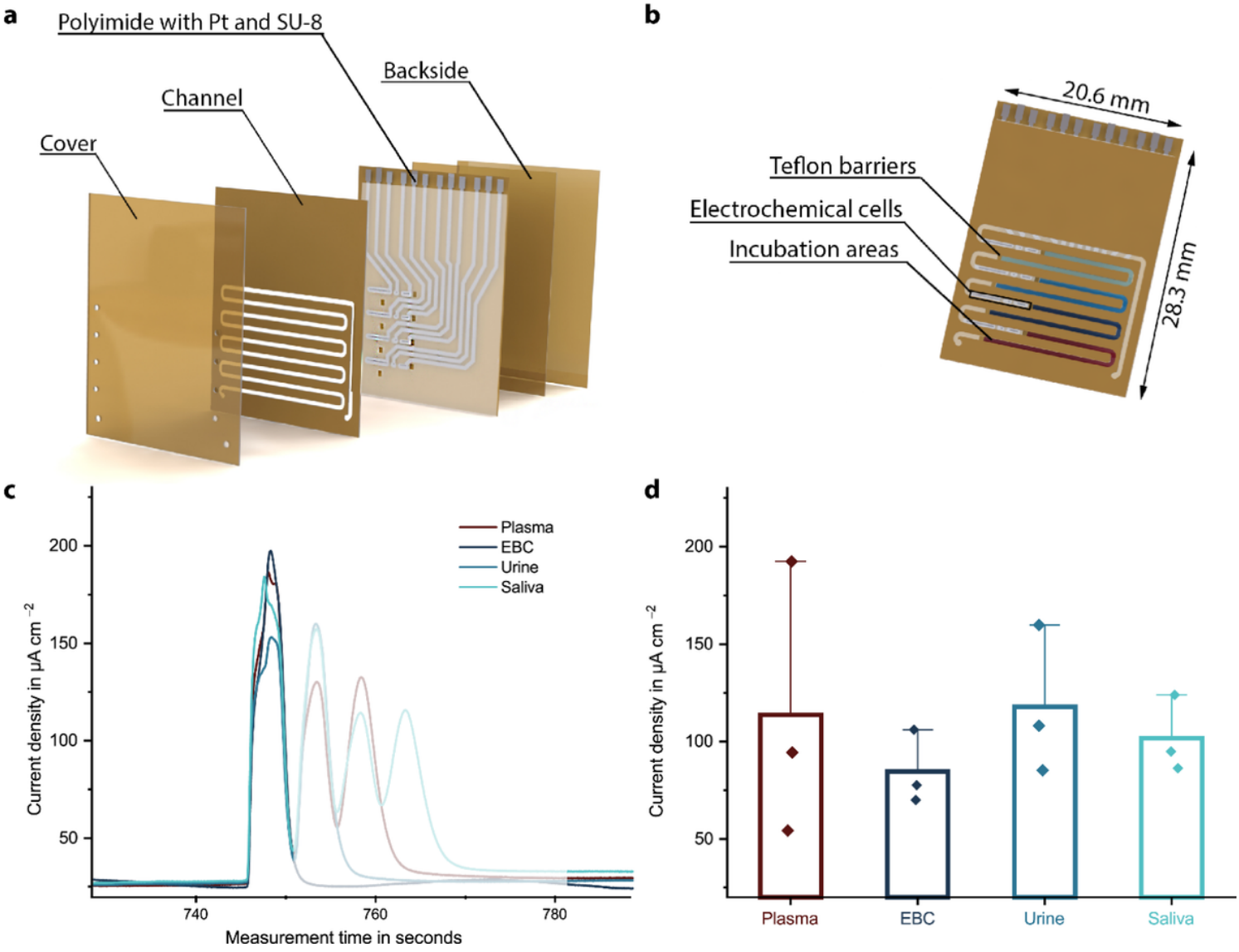

Figure 5

Multianalyte/sample capability of the proposed biosensing technology. (a) 3D rendering of the stacked multiplexed biosensor (Biosensor X) and (b) four different incubation areas, individual electrochemical cells and Teflon barriers preventing electrode fouling. (c) Amperometric signal readout. The first four successive peaks correspond to the accumulation of electrochemically active species in the immobilization area during stop-flow protocol. During the “flow” phase, these species are passing through neighboring electrochemical cells in addition to their own individual electrochemical cell, which creates the following faint peaks. (d) Demonstration of the proof of principle via measuring four different sample types on the single-channel multiplexed biosensor. Box and whisker plot for n = 3 replicates. Error bars represent the outlier range.

Supplementary Files

This is a list of supplementary files associated with this preprint. Click to download.

- Biosensorenabledonsitetherapeuticdrugmonitoringofantibiotics_SupportingInformation.docx